

Growth of rare-earth monolayers on synthetic fluorine mica

F. Tsui, P. D. Han, and C. P. Flynn

University of Illinois at Urbana-Champaign, 1110 West Green Street, Urbana, Illinois 61801

(Received 8 September 1992)

We have grown single-crystal rare-earth films on cleaved faces of synthetic fluorine mica fluorophlogopite by molecular-beam-epitaxy techniques. This has made it possible to measure material properties such as magnetism in monolayer structures.

I. INTRODUCTION

Epitaxial growth is a technique of widely recognized value for the synthesis of material configurations and the creation of controlled material properties. A common limitation is set by the substrate template required for the growth of the desired structure. The problem is that the substrate is generally much thicker than the sample grown upon it, and may therefore interfere with properties of, or measurements made on, the epitaxial film. Thus a metallic substrate causes problems with conductivity measurements, and bulk characteristics of a thick substrate may overwhelm those of the thin film, as in optical or dielectric measurements.

In this paper we point out the special advantages of synthetic fluorine mica fluorophlogopite as a substrate material for use in epitaxial growth when the interference of bulk substrate properties with subsequent measurements could otherwise become a serious problem. Natural mica, for example ruby muscovite, has long been employed as a substrate for thin-film deposition. It has the chemical advantage of being relatively inert, and as a transparent insulator is suitable for optical and conduction measurements over wide ranges of epilayer properties. Of particular note here is that mica is readily cleaved down to thickness of several μm , so that the substrate volume can often be reduced to a value comparable to that of the epilayer. This is not the case for many widely used substrate materials such as sapphire or silicon. On the negative side, mica provides only a weak structural template, owing to its smooth surface and saturated bonding, and is difficult to maintain macroscopically flat when it is very thin (although this may not detract from its serviceability, for example in conductivity applications). A serious deficiency of natural mica, for example muscovite, is its high reactivity at elevated temperatures, and, disastrously, chemical decomposition and spontaneous exfoliation take place at temperatures above about 800 K due to OH losses. This temperature is low enough to prevent the growth of chemical buffers such as Nb, which are a commonly used link in the synthesis chain for metals on sapphire. The striking advantage of the synthetic mica is that it remains stable at temperatures up to 1400 K,¹ and therefore accommodates the growth of valuable chemical buffer layers such as Nb and Ir, which require growth temperatures above 1100 K if single-crystal samples of good quality are to be achieved.²

A particular application of synthetic mica substrates to the measurement of magnetism in monolayer structures is described in what follows. This provides an apt illustration of a case in which high growth temperatures are required simultaneously with a controlled substrate magnetism. Either too large a substrate volume, or a significant problem with magnetic impurities, makes the desired measurements impractical. Section II of the paper reviews the synthesis of the mica employed in this work and its characteristics. Section III illustrates its use in epitaxial growth by the example of reactive rare-earth metals grown on an initial niobium buffer layer. Section IV describes how the resulting sensitivity in magnetic measurements makes accurate measurements of the magnetism of monolayer epitaxial systems directly accessible. The results are summarized in Sec. V.

II. GROWTH AND PROPERTIES OF SYNTHETIC FLUORINE MICA

Fluorophlogopite, $\text{KMg}_3(\text{AlSi}_3\text{O}_{10})\text{F}_2$, is an important member of the fluorine mica family, which is composed of a wide variety of isomorphically substituted fluoromicas. Natural mica, on the other hand, such as muscovite $\text{KAl}_2(\text{AlSi}_3\text{O}_{10})(\text{OH})_2$ or phlogopite $\text{KMg}_3(\text{AlSi}_3\text{O}_{10})(\text{OH})_2$, contains hydroxyl ions, OH^- , instead of F^- ions. By fully substituting F^- ions for OH^- ions in the lattice of natural phlogopite, one obtains fluorophlogopite. The much stronger bonding force of F^- ions relative to that of the OH^- ions gives rise to the much more stable structure of fluorophlogopite. Due to its congruent melting under normal atmospheric conditions, fluorophlogopite can be synthesized by melting suitable batch materials using various techniques.

Synthesis of fluorophlogopite has been studied for many decades.³ The internal resistance electrical melting technique⁴ is perhaps the basic method for synthesizing a large amount of fluorophlogopite. A furnace used in the internal resistance electrical melting process consists of a shell to contain a batch, a pair of electrodes positioned to generate heat at the interior of the batch, and a power supply. The starting composition of the batch is a nearly stoichiometric mixture of K_2O , MgO , Al_2O_3 , SiO_2 and fluorides with a small amount of excess F^- to balance the F^- loss in the melting process. Mica crystals are formed from the melt through a slow cooling process, and mica sheets of size $0.5-1.5 \times 50 \times 60 \text{ mm}^3$ can be mechanically

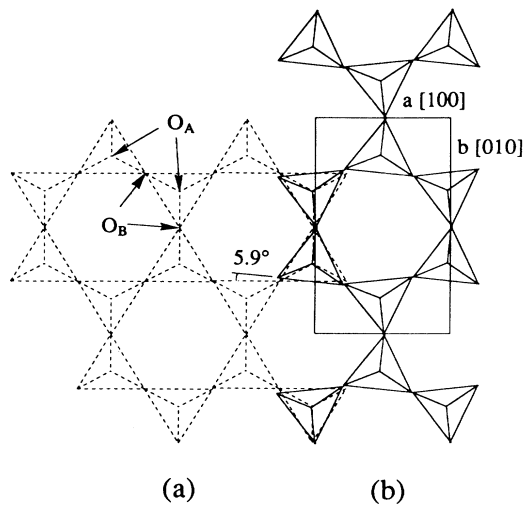


FIG. 1. Surface layer of the synthetic mica fluorophlogopite (Ref. 1).

separated from the solidified material. However, larger single crystals, used in the thin-film growth reported here, are synthesized by a special seeded-Bridgman-Stockbarger technique¹ that uses mica flakes, produced by the above techniques, as raw materials. Mica flakes and seeds are carefully placed in the platinum crucibles inside a furnace equipped with computer-controlled MoSi₂ heating elements. Booklike single crystals with dimensions of 10×100×200 mm³ can be obtained by this technique.

The unit cell of fluorophlogopite is 2KMg₃(AlSi₃O₁₀)F₂ with a monoclinic structure. It belongs to *C2/m* space group. The lattice parameters are $a = 5.308(2) \text{ \AA}$, $b = 9.183(3) \text{ \AA}$, $c = 10.139(1) \text{ \AA}$, and $\beta = 100.07(2)^\circ$. Like other layered silicates, mica crystals contain pseudohexagonal Z₂O₅ sheets (Z=Si and Al) formed by ZO₄ tetrahedrons. Each tetrahedron contains three shared ions and one unshared oxygen ion at its corners, as illustrated in Fig. 1. The unshared apical oxygen ions O_A lie in one plane and the shared basal oxygen ions O_B lie in another. F⁻ ions are coplanar with the apical oxygen ions located at the center of the hexagons defined by these oxygen ions. Two Z₂O₅ sheets and the associated F⁻ ions, each with their apical oxygen ions directed toward each other, are bonded by the Mg cations to form a mica layer. Mica layers themselves are

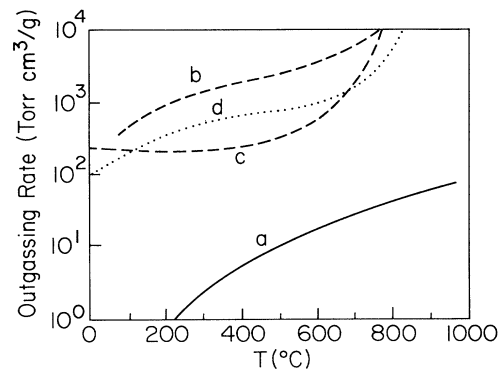


FIG. 2. High-temperature outgassing rate for different micas, (a) the synthetic fluorine mica and (b)–(d) several natural micas (Ref. 1).

loosely bonded to each other by the relatively large K⁺ cations between the basal oxygen ions.

Due to the weak bonds between the K⁺ ions and the basal oxygen ions, mica can be perfectly cleaved along K⁺ planes on {001} surfaces into thin sheets of a few μm thick with atomically smooth surfaces. The cleaved mica surface therefore contains the exposed potassium ions and the basal oxygen ions. We note that Z₂O₅ sheets, rather than having hexagonal symmetry [Fig. 1(a), dashed tetrahedrons], actually possess a di-trigonal symmetry [Fig. 1(b), solid tetrahedrons]. The amount of deviation of the di-trigonal symmetry from the hexagonal one is determined to be 5.9°.⁵

Finally, it is well established that the replacement of the OH⁻ ions in natural mica by the F⁻ ions gives the synthetic fluorine mica a much higher maximum operation temperature.¹ Its degassing rate at 900 °C is ~2000 times lower than the natural counterparts, as shown in Fig. 2. These high-temperature properties, together with the relatively high purity, make fluorophlogopite a suitable substrate for molecular-beam-epitaxy (MBE) growth. Natural mica, on the other hand, usually contains 6–8 % of Fe, Na, Ca, Ta, Li, . . . impurities. The important physical properties of various micas are summarized in Table I.

III. EPITAXIAL GROWTH OF RARE-EARTH METALS ON SYNTHETIC FLUORINE MICA

The heavy rare-earth metals present a typical series of problems for epitaxial growth. In fact, the problems can

TABLE I. Physical properties of fluorophlogopite and natural micas (Ref. 1).

Physical properties	Natural muscovite	Natural phlogopite	Synthetic fluorophlogopite
Density (g/cm ³)	2.7–2.9	2.7–2.85	2.78–2.85
Maximum operation temperature (°C)	550	850	1100
Melting point (°C)	Decomposes	Decomposes	1378
Water constitution	4.5%	3.2%	None

be accommodated but not fully resolved. With difficulty these important hcp magnetic metals can be grown by homoepitaxy⁶ in all principal orientations. By a much-used synthesis route starting from sapphire (11 $\bar{2}$ 0) with a Nb (100) buffer,^{2,7} they can be grown on their basal (0001) planes. Neither route is suitable for sensitive magnetic measurements owing to the resulting large magnetic background from the substrate, as described in Sec. I. Substrates cleaved from alternative insulators such as MgO present much the same difficulties. Neither natural nor synthetic mica can be employed with rare-earth metals directly at their growth temperature near 700 K because they react to form completely spoiled films. Buffers such as Nb or Mo grow satisfactory only at temperatures well above the exfoliation temperature (900 K) of natural mica, so this route also is blocked.

We find that Nb(100) grows smoothly on (001) cleaved fluorophlogopite at about 1100 K. The procedure was to cleave the mica in distilled-deionized water and introduce it immediately into the MBE chamber without further surface preparation. For this purpose the mica was held on the metal heater by clamped wires. Thin mica is of course extremely flexible. For large sheets thermal contact between the epilayer and the substrate heater is poor. This presents less problem in the regime near 1100 K of Nb growth, where radiative coupling is strong, than at 700 K, where conduction also is important. In a typical procedure the chamber was pumped down to the 10⁻¹⁰-torr range at room temperature, and then degassed at 1200 K for 30 min, before buffer growth was undertaken.

A further critical problem arises from the weak template effect offered by mica. For hexagonal substrates it is frequently observed⁸ that the symmetry is echoed in subsequent epilayers, presumably because of hexagonal local nucleation. This is not the case for Nb on mica, where the strong (110) habit of the epilayer apparently overcomes the hexagonal template near 1100 K. The result is a smooth film of Nb (110) domains, each about 300 Å in diameter, and occupying equally the three equivalent {110} orientations available on the mica (001) surface. A buffered single-crystal surface for further growth processes thus remains lacking.

For present purposes the lack of a perfect buffered substrate can be handled by simply proceeding with the rare-earth growth on the Nb domain structure. In the present experiments Y was employed as the "rare-earth" seed layer, and grown typically 0.1 μm thick. Figure 3 is

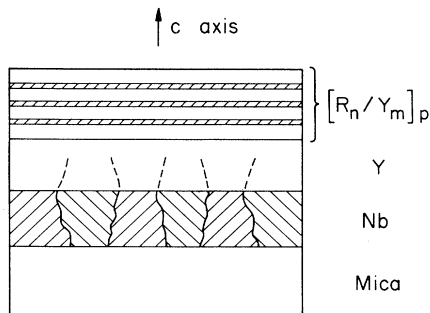


FIG. 3. Schematic diagram of the sample structure grown on synthetic mica substrate.

a sketch of the resulting sample structures. What apparently happens is that Y (0001) nucleates separately on the differently oriented Nb domains. Since, however, the domains are related to each other by $\pi/3$ rotations, the hexagonal Y domains are indistinguishable other than by in-plane translations related to the Nb domains. With continued Y growth, the Y structural faults that derive from the Nb domain boundaries gradually grow out and are eliminated to produce a reasonably-high-quality Y (0001) single crystal on which magnetic rare-earth systems of equivalent quality could then be prepared. Our x-ray-diffraction experiments indicate that the crystal coherence length for Y is > 500 Å along the [0001] growth direction and > 300 Å in the growth plane. In the present research the Y quality never appeared to reach the very high levels accessible by direct preparation from sapphire (11 $\bar{2}$ 0) with a Nb (110) single-crystal buffer. However, the differences were not large and cer-

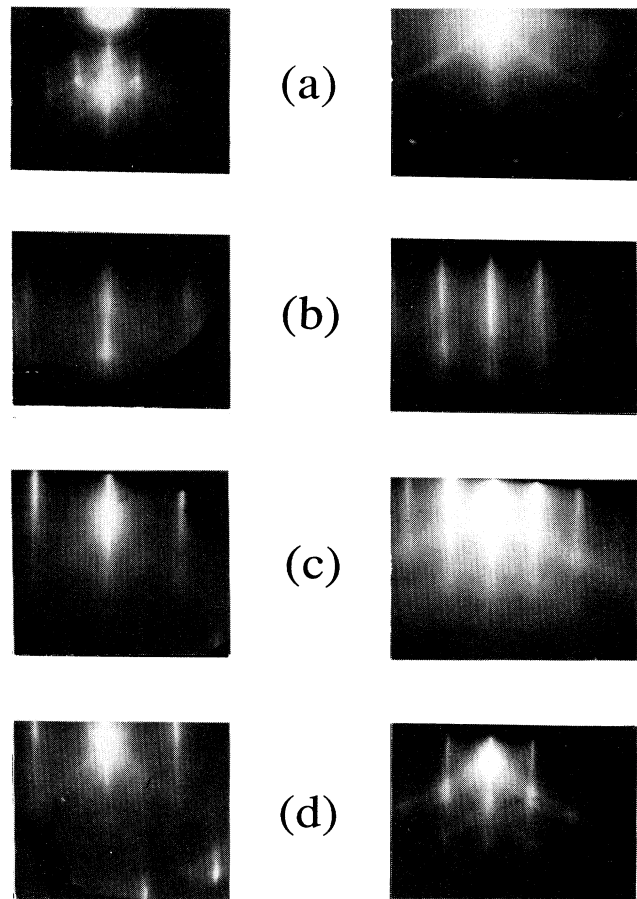


FIG. 4. (a)–(c) The RHEED patterns of (0001) Y grown on (001) synthetic mica using (110) Nb as a buffer layer, showing the 30° rotation between the symmetry directions of Y and mica (0001) surfaces; (a) left, along the mica [010] azimuth; right, along the mica [100] azimuth; (b) left, along the one of the [100] azimuths of Nb; right, along one of the [110] azimuths; and (c) left, along the [1120] azimuth of the Y surface; right, along the [1100] azimuth. (d) As a comparison, the Y surface grown on sapphire, is shown.

tainly have minimal influence on the magnetic measurements described in Sec. IV, since the crystal coherence length is much longer than the known magnetic interaction range. Illustrative reflection-high-energy-electron-diffraction (RHEED) patterns for mica, the Nb (110) domains, the resulting (0001) Y, and a comparison with Y on sapphire are presented in Fig. 4.

As indicated in Fig. 4, Y (0001) epitaxy on (110) Nb follows the expected Nishiyama-Wasserman relationship⁷ with the $[11\bar{2}0]$ direction of the Y lattice parallel to the $[001]$ direction of the Nb. The three (110) Nb domains on (001) mica do not, however, follow the same relationship. Instead, the $[001]$ directions of the Nb lattice lie parallel to the $[010]$ direction of the mica. Other bcc transition metals, such as Mo and Ta, also grow the same way. As a result the symmetry axes of the (0001) Y film are rotated by 30° from those of the (001) mica surface.

We have also grown fcc metals, such as Rh, Ir, Pt, and Au on synthetic fluorine mica. They grow in the $[111]$ orientation. Because these materials form microcrystalline compounds with Y at the Y growth temperature,⁹ they are not suitable as buffer materials for the rare-earth metals.

IV. MAGNETIC MEASUREMENTS

The magnetization M of samples studied in the present research was determined by means of a commercial superconducting-quantum-interference-device (SQUID) system, Quantum Design MPMS. Its typical characteristics include an absolute detection limit of $M = 10^{-8}$ emu, and a fractional reproducibility of 1% set mainly by the reproducibility of the field, including the sample position. Samples of maximum volume 0.05 cc were contained in a thin gelatin ampoule and supported by a plastic straw. Together these contribute a magnetization of -2×10^{-5} emu at a typical working field of 1 kOe, for a limiting uncertainty of 10^{-6} emu in magnetization. To the extent that substrate magnetism causes negligible uncertainties, this sets a detection limit of 10^{14} fully polarized Gd spins, which occupy a surface area of about 0.1 cm^2 . In practice, a $10\text{-}\mu\text{m}$ -thick mica substrate for this film would contribute a magnetization of 10^{-8} emu, and therefore introduce an uncertainty of 10^{12} fully polarized Gd spins at the working field. From these illustrative figures it may be deduced that one monolayer sensitivity for strongly polarized Gd requires a sample area of 0.1 cm^2 , and that 1% precision accordingly requires 10 cm^2 . As a practical matter, about 10 cm^2 of mica and epilayer may readily be packed into the available capsules.

The temperature and field dependences of the magnetization for the synthetic mica are presented in Fig. 5. The magnetization is that of a typical diamagnetic silicate, but with a large paramagnetic contribution due to the relatively high level of ferromagnetic impurities. Its temperature dependence has a Curie law rise near 0 K, and its field dependence is that of a paramagnet and diamagnet mixture, with a small ferromagnetic moment indicated by a peak at $\sim 2 \text{ kOe}$ field at high temperatures. The observed small ferromagnetism probably arises from ferromagnetic clusters, similar to the origin of the overall paramagnetism.

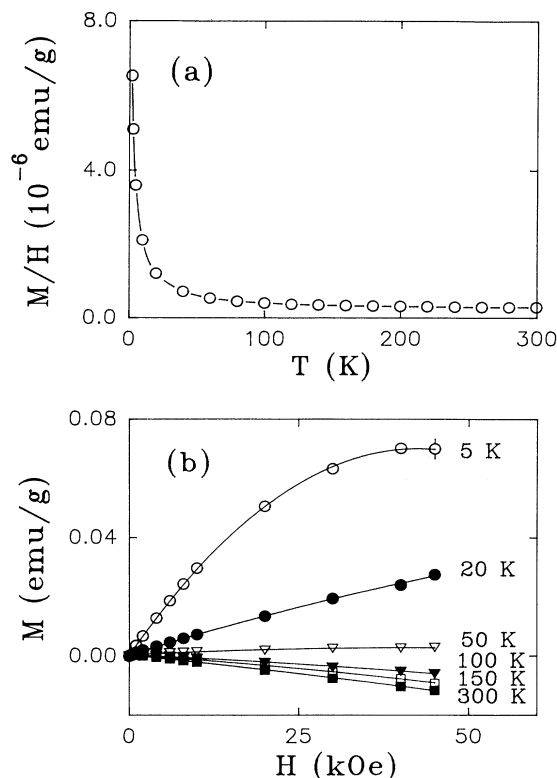


FIG. 5. (a) The temperature-dependent magnetization at a field of 1 kOe for the synthetic fluorine mica and (b) the field dependence of the magnetization at various temperatures.

With regard to the interesting problem of investigating magnetic characteristics of two-dimensional (2D) systems, the following general comments may be offered. Studies may concern either 2D structures located on surfaces or 2D layers buried in the bulk. From a theoretical standpoint there is no distinction in principle between these two alternative geometries, and indeed the buried system offers the merit of a more uniform environment for the spins, particularly at submonolayer coverages. Still greater advantages accrue in practice for buried layers. One important factor is that the buried layer is naturally protected from environmental contamination and degradation, so that the magnetic system at least may retain its pristine state upon removal from the synthesis chamber. A second factor of great practical significance is that magnetic interactions along the growth direction are generally limited to some finite range which can be determined by direct experimentation. For buried layers this introduces the possibility that the unit layer may be repeated many times inside the epilayer, with successive repeats separated by a distance exceeding this interaction range, thereby enhancing the magnetic signal by a factor equal to the number of repeats in the sample. For the rare-earth metals in Y the coupling range along $[0001]$ deduced in earlier research falls below 1 mK about 150 \AA .^{7,10} Repeats of up to 60 buried layers at $200\text{-}\text{\AA}$ intervals were therefore employed in the present research to enhance the accuracy of magnetic measurements on the more-dilute samples. Thus the structures took on the su-

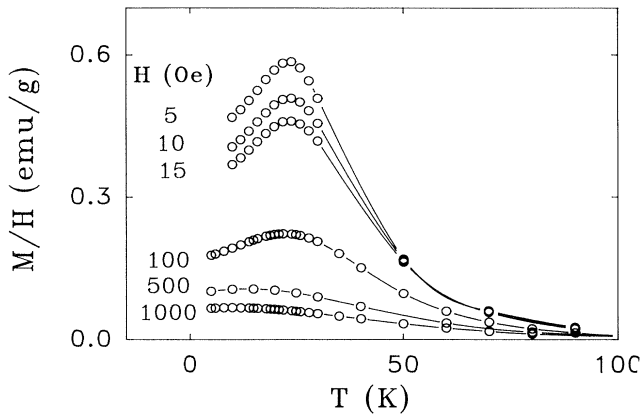


FIG. 6. Temperature dependence of the magnetization in $\frac{1}{2}$ of a monolayer Gd at various fields applied perpendicular to the c axis.

per lattice form shown in Fig. 3, while the magnetism remained that of isolated 2D systems, at least in the temperature range of the present studies.

To illustrate the sensitivity of the technique, the temperature dependence of the magnetization for a sample

with $\frac{1}{2}$ of a monolayer Gd in Y grown on synthetic mica is presented in Fig. 6. At low temperatures the field-cooled susceptibility goes through a distinct maximum, which is generally identified with the onset of spin-glass freezing. The result shown in Fig. 6 clearly demonstrates that we can easily detect much less than $\frac{1}{100}$ of the Gd saturation moment at a small fractional monolayer coverage. The magnetic results from these monolayer and submonolayer systems will be reported elsewhere.

V. SUMMARY

In this paper we describe the advantages of synthetic mica fluorophlogopite as a substrate for epitaxial growth of films. Principal among these advantages is that this material can be employed for buffer layer growth at temperatures up to 1400 K. At the same time it is relatively inert to chemical reaction, and may be cleaved thin to reduce the bulk substrate interference with property measurements. The example of magnetic measurements at submonolayer sensitivity is described in the text.

ACKNOWLEDGMENTS

This research was supported in part by NSF Contract No. DMR-88-208888.

- ¹G. F. Wang and P. D. Han, in *Crystal Growth*, edited by K. C. Zhang and L. H. Zhang (Chinese Scientific, Beijing, 1980), pp. 500–561.
- ²S. M. Durbin, J. E. Cunningham, and C. P. Flynn, *J. Phys. F* **12**, L75 (1982).
- ³R. S. Haskiel and H. I. Kenneth, *Fluorine Mica*, Bureau of Mines, U.S. Dept. of the Interior, Bulletin No. 647 (U.S. GPO, Washington, DC, 1969).
- ⁴R. A. Humphrey, U.S. Patent No. 2,711,435 (21 June 1955).
- ⁵J. W. McCauley, R. E. Newnham, and G. V. Gibbs, *Am. Mineral.* **58**, 249 (1973).
- ⁶F. Tsui, C. P. Flynn, M. B. Salamon, R. W. Erwin, J. A. Borch-

- ers, and J. J. Rhyne, *Phys. Rev. B* **43**, 13 320 (1991).
- ⁷J. Kwo, D. B. McWhan, E. M. Gyorgy, L. C. Feldman, and J. E. Cunningham, in *Layered Structures, Epitaxy, and Interfaces*, edited by J. M. Gibson and L. R. Dawson, MRS Symposia Proceedings No. 37 (MRS, Pittsburgh, 1985).
- ⁸J. C. A. Huang, R. Du, and C. P. Flynn, *Phys. Rev. Lett.* **66**, 341 (1991).
- ⁹T. B. Massalski, *Binary Alloy Phase Diagrams* (American Society for Metals, Metals Park, OH, 1986).
- ¹⁰J. J. Rhyne, R. W. Erwin, J. A. Borchers, M. B. Salamon, R. Du, and C. P. Flynn, *J. Appl. Phys.* **61**, 4043 (1987).

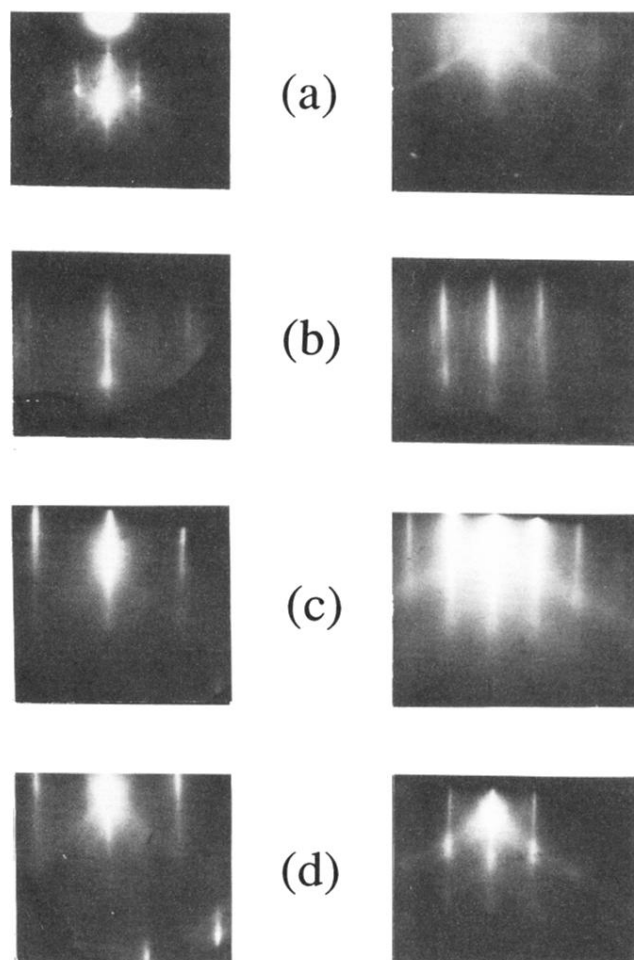


FIG. 4. (a)–(c) The RHEED patterns of (0001) Y grown on (001) synthetic mica using (110) Nb as a buffer layer, showing the 30° rotation between the symmetry directions of Y and mica (0001) surfaces; (a) left, along the mica [010] azimuth; right, along the mica [100] azimuth; (b) left, along one of the [100] azimuths of Nb; right, along one of the [110] azimuths; and (c) left, along the $[11\bar{2}0]$ azimuth of the Y surface; right, along the [110] azimuth. (d) As a comparison, the Y surface grown on sapphire, is shown.